Nonlinear dynamical triggering of slow slip on simulated earthquake faults with implications to Earth

P. A. Johnson,[1] B. Carpenter,[2] M. Knuth,[3] B. M. Kaproth,[2] P.-Y. Le Bas,[1] E. G. Daub,[1,4] and C. Marone[2]

Received 5 July 2011; revised 23 February 2012; accepted 6 March 2012; published 21 April 2012.

[1] Among the most fascinating, recent discoveries in seismology are the phenomena of dynamically triggered fault slip, including earthquakes, tremor, slow and silent slip—during which little seismic energy is radiated—and low frequency earthquakes. Dynamic triggering refers to the initiation of fault slip by a transient deformation perturbation, most often in the form of passing seismic waves. Determining the frictional constitutive laws and the physical mechanism(s) governing triggered faulting is extremely challenging because slip nucleation depths for tectonic faults cannot be probed directly. Of the spectrum of slip behaviors, triggered slow slip is particularly difficult to characterize due to the absence of significant seismic radiation, implying mechanical conditions different from triggered earthquakes. Slow slip is often accompanied by nonvolcanic tremor in close spatial and temporal proximity. The causal relationship between them has implications for the properties and physics governing the fault slip behavior. We are characterizing the physical controls of triggered slow slip via laboratory experiments using sheared granular media to simulate fault gouge. Granular rock and glass beads are sheared under constant normal stress, while subjected to transient stress perturbation by acoustic waves. Here we describe experiments with glass beads, showing that slow and silent slip can be dynamically triggered on laboratory faults by ultrasonic waves. The laboratory triggering may take place during stable sliding (constant friction and slip velocity) and/or early in the slip cycle, during unstable sliding (stick-slip). Experimental evidence indicates that the nonlinear-dynamical response of the gouge material is responsible for the triggered slow slip.

Citation: Johnson, P. A., B. Carpenter, M. Knuth, B. M. Kaproth, P.-Y. Le Bas, E. G. Daub, and C. Marone (2012), Nonlinear dynamical triggering of slow slip on simulated earthquake faults with implications to Earth, *J. Geophys. Res.*, *117*, B04310, doi:10.1029/2011JB008594.

1. Introduction

[2] Accumulating evidence suggests that dynamic triggering of fault slip takes place in most or all of the identified spectrum of slip behaviors for tectonic faults [*Peng and Gomberg*, 2010]. It is currently thought that a large percentage of earthquake aftershocks may be dynamically triggered [*van der Elst and Brodsky*, 2010; *Marsan and Lengliné*, 2008] and it is therefore plausible that large numbers of all types of fault slip events are dynamically triggered. Dynamic triggering can take place in close proximity to the earthquake main shock [*Gomberg et al.*, 2003; *van der Elst and Brodsky*, 2010; *Taira et al.*, 2009] or remotely at great distances from the triggering source, and it may be either instantaneous or, more frequently, delayed [*Gomberg et al.*, 2004; *Bodin et al.*, 1994; *Gomberg*, 2001]. Instantaneous dynamic triggering of slip is associated primarily with surface waves [*Bodin et al.*, 1994; *Gomberg*, 2001], and occasionally shear waves (e.g., D. Zigone et al., Triggering of tremors and slow slip event in Guerrero (Mexico) by the 2010 *Mw* 8.8 Maule, Chile, earthquake, submitted to *Geophysical Research Letters*, 2012), while delayed triggering may be due to dynamically induced instability [*Johnson and Jia*, 2005; *Johnson et al.*, 2008; *Griffa et al.*, 2011, 2012] and/or cascading or avalanche behavior [e.g., *Sornette and Sornette*, 1989]. Triggering strains can be surprisingly low ($<10^{-8}$) [e.g., *van der Elst and Brodsky*, 2010], inducing extremely small displacements (a strain of 10^{-8} produced by a typical surface wave generates a particle displacement of order 30 microns at earthquake nucleation depths). As triggering of earthquakes occurs via small stress perturbations, a logical conclusion is that faults are in a critical state, already near failure [e.g., *Scholz*, 2010; *Johnson and Jia*, 2005] and the wave

[1]Geophysics Group, Los Alamos National Laboratory, Los Alamos, New Mexico, USA.
[2]Department of Geosciences, Pennsylvania State University, University Park, Pennsylvania, USA.
[3]Department of Geology and Geophysics, University of Wisconsin-Madison, Madison, Wisconsin, USA.
[4]Center for Nonlinear Studies, Los Alamos National Laboratory, Los Alamos, New Mexico, USA.

0148-0227/12/2011JB008594

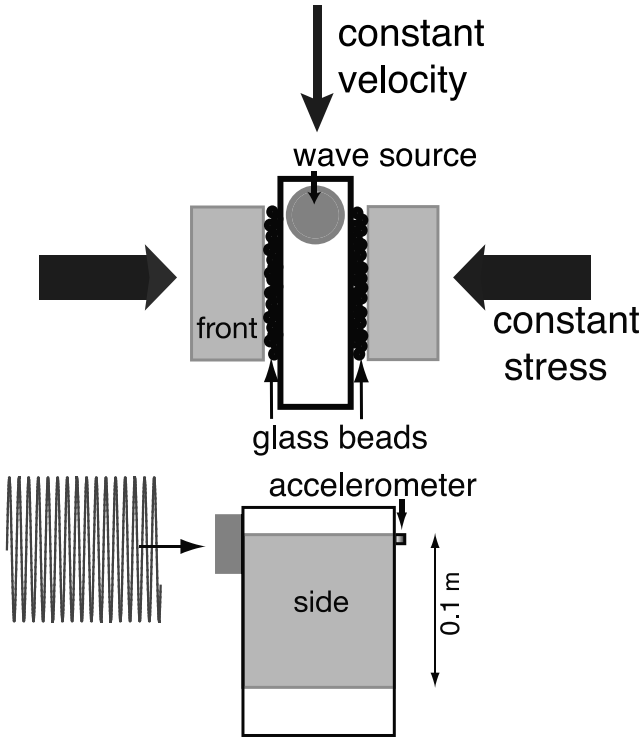

Figure 1. Experimental configuration. We employ a double-direct shear configuration in a biaxial load frame, which applies a normal stress to three steel forcing blocks that contain symmetric layers of glass beads at the block interfaces. An orthogonal piston drives the central block downward at a constant displacement rate to create shear. The steel blocks have rough surfaces in contact with the glass beads. The wave source transducer and the accelerometer are placed on opposite sides of the central block.

perturbation advances or delays the time of slip [e.g., *Gomberg et al.*, 1997].

[3] Shallow, dynamically triggered slow slip, observed geodetically, has been known for several decades [*Allen et al.*, 1972; *Bodin et al.*, 1994]. Some observations of triggered slow slip, particularly shallow slow slip, have been shown to take place at any time in the earthquake cycle by *Hudnut and Clark* [1989]. *Gomberg* [2010] has recently argued that slow slip associated with nonvolcanic tremor must be in a near-failure condition. In both cases, the presence of slow slip suggests lower effective stress conditions than earthquakes [*Brodsky and Prejean*, 2005], a very weak fault [*Zoback and Beroza*, 1993] and/or chemical and thermal conditions not well understood. In the event that seismicity is recorded for a dynamically triggered slow slip, it is very small in magnitude and can be delayed from the slip event onset [*Glowacka et al.*, 2002; *Bodin et al.*, 1994]. Triggered slow slip may last from minutes to months, be delayed and/or occur repeatedly in sequence [*Bodin et al.*, 1994; Zigone et al., submitted manuscript, 2012]. Recently, dynamically triggered slow and silent slip has been broadly observed simultaneously with nonvolcanic tremor [*Rogers and Dragert*, 2003; *Hiramatsu et al.*, 2008; *Miyazawa and Mori*, 2005; *Miyazawa and Brodsky*, 2008; *Brodsky and Prejean*, 2005; *Itaba and Ando*, 2011; Zigone et al., submitted manuscript, 2012]. Tidal forces were shown to drive non-volcanic tremor [*Hawthorne and Rubin*, 2010], showing that oscillatory loads at much lower frequencies than seismic waves can trigger tremor and slow slip. These observations imply specific physical constraints regarding triggering of slow slip, and open a new portal into deep crustal slip mechanics as many have noted [e.g., *Rubinstein et al.*, 2010].

[4] A number of observations show dependence of earthquake triggering on the amplitude of the triggering seismic waves, suggesting a nonlinear dynamical mechanism with a seismic strain-amplitude threshold [*Johnson and Jia*, 2005; *Gomberg and Johnson*, 2005], as well as strong directional effects of the triggering wave [e.g., *Gonzalez-Huizar and Velasco*, 2011; *Gomberg et al.*, 2004; Zigone et al., submitted manuscript, 2012]. Because triggered slow slip may occur at lower effective pressures and/or on weaker faults than earthquake triggering, it may well be more susceptible to nonlinear dynamical effects. Indeed, in Japan, amplitude-dependent triggered-tremor associated with slow slip that may be nonlinear in nature has been recently observed in response to the 2004 Sumatra-Andaman and 2003 Tokachi-oki earthquakes [*Miyazawa and Brodsky*, 2008]. Observations of triggering by the 2002 Denali earthquake show evidence for amplitude dependence with the triggering surface waves [*Rubinstein et al.*, 2007]. Triggering of slow slip and tremor at Guerrero, Mexico also suggest dynamic wave amplitude dependence (Zigone et al., submitted manuscript, 2012).

[5] To date, our laboratory studies show that dynamic triggering requires the presence of gouge material—the granular material in the fault core that is created by frictional wear and comminution associated with granular crushing and grinding during repeated episodes of slip over geologic time. We have not succeeded in dynamically triggering slip along bare rock faces or for frictional shear between other types of solid interfaces, such as Plexiglas. Because gouge may be a necessary ingredient for triggering of slip along tectonic faults, it is important to understand the physics of gouge friction under seismogenic conditions. In this article, we experimentally investigate triggered slow slip in a system that contains a mock gouge material, and show that nonlinear dynamics play a key role in the slip process.

2. Experiments

[6] We perform experiments in a double-direct shear configuration using a servo-hydraulic testing machine (Figure 1) [e.g., *Marone*, 1998]. Layers of simulated fault gouge are subjected to shear under conditions of constant normal stress with periodic application of acoustic waves. The apparatus is servo-controlled so that constant normal load and shear displacement rate are maintained at ± 0.1kN and ± 0.1 μm/s, respectively. The applied stresses on the shearing layers are measured with strain gauge load cells in series with each of the loading axes. The apparatus is monitored via computer to record loads, displacements, and stresses at 10 kHz sampling frequency. A second acquisition system records acoustic acceleration, shear stress and layer thickness at 330 kHz sampling frequency. The initial layer thickness is 2×4 mm (two layers), the frictional contact

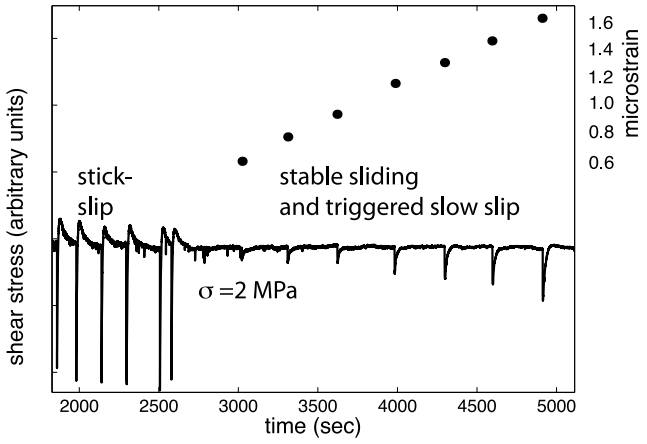

Figure 2. Strain amplitudes of applied acoustic perturbation detected at accelerometer (solid circles) and shear stress (solid line) versus experimental run time for an experiment run at 2 MPa horizontal stress. The stick slip and stable sliding regimes are both shown. At the time of each acoustical perturbation there is a shear stress drop, as well as a thickness change and a shear displacement (Figure 4). Post disturbance, there is a long-term recovery back to the equilibrium shear stress over tens of seconds. Figure 3 shows an expanded view of the triggered slow slip occurring at 4595 s. Figure 4 compares the slow slip events with one stick-slip event.

dimensions is 10x10 cm, and the central block vertical displacement rate is 5 μm /s, corresponding to a strain rate of approximately 1.2×10^{-3}/s. In the experiments presented here, applied horizontal stress is 2 MPa. The beads are class IV spheres (dimension from 105 to 149 microns). For triggering, a toneburst of ~5 s at 40.3 kHz is applied via an acoustic source (Figure 1). A Matec M50-2, 50 kHz piezoceramic is attached mechanically to the central block using vacuum grease as couplant and driven by a Techron 7520 amplifier. The signal is detected on the opposite face of the central block using a Brüel and Kjær model 4393 accelerometer attached with beeswax, amplified by a Brüel and Kjær 2635 charge amplifier. Elastic wave strain is estimated as follows. In a harmonic wave, strain $\varepsilon = du/dx$ is related to acceleration $\ddot{u} = d^2u/dx^2$

$$\varepsilon = \frac{\ddot{u}}{\omega c} = \frac{\dot{u}}{c} \tag{1}$$

for the time-averaged amplitude. We digitize the acceleration data and record the absolute value of the sinusoidal waveform with a sampling rate of 330 kHz at 16 bits vertical resolution. Calculated detected strain amplitudes applied range from about 0.01–9 microstrain, corresponding to <1% of the normal stress. Background noise is $<5 \times 10^{-7}$ strain with frequency <100 Hz. Noise is removed by high-pass filtering the data above 100 Hz.

[7] We use an amplitude thresholding algorithm to extract acoustic emissions after band pass filtering the signal at 34–45 kHz. Visual inspection of the time signals shows that the algorithm misses very few acoustic emission events (≪1%).

3. Results

[8] We find that slow and silent-slip is triggered by dynamic waves when the normal stress is ≤~3 MPa under room dry conditions. Weak acoustic emissions (AE) accompany and follow the slow slip event. In general, at larger normal loads acoustic waves trigger primarily dynamic stick-slip failure (triggered laboratory earthquakes) with attendant seismic wave radiation [*Johnson et al.*, 2008]. For the range of normal stresses from 0.5 to 3 MPa load, laboratory earthquake stick-slip cycles and stable sliding are interspersed, and triggering may be induced either during stick-slip or stable frictional sliding. A fundamental test of nonlinear dynamics in the triggering process is amplitude dependence of measured physical parameters that include shear stress drop, thickness change and displacement along the shearing axis. Experiments with prolonged stable sliding provide a means to explore the amplitude dependence of dynamic-wave triggering of slow slip because the reference shear stress, material thickness and displacement-rate are constant. Thus the amplitude dependences of measured parameters are simple to measure relative to the reference state (Note the two gouge layers thin very slowly as material is lost at the bottom

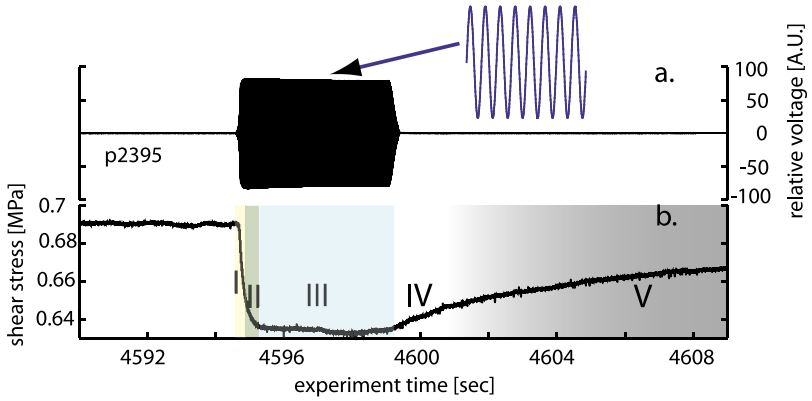

Figure 3. Example of triggered slow slip in the laboratory. (a) The triggering toneburst signal recorded using the accelerometer, in arbitrary units (A.U.). The sampling frequency is 330 kHz, the signal has a center frequency of 40.3 kHz, and is applied for approximately 5 s duration. The inset shows a zoom of the recorded signal (~200 microseconds). (b) The shear stress signal. When the toneburst is applied at about 4595 s there are five characteristic stages that follow, as described in the text.

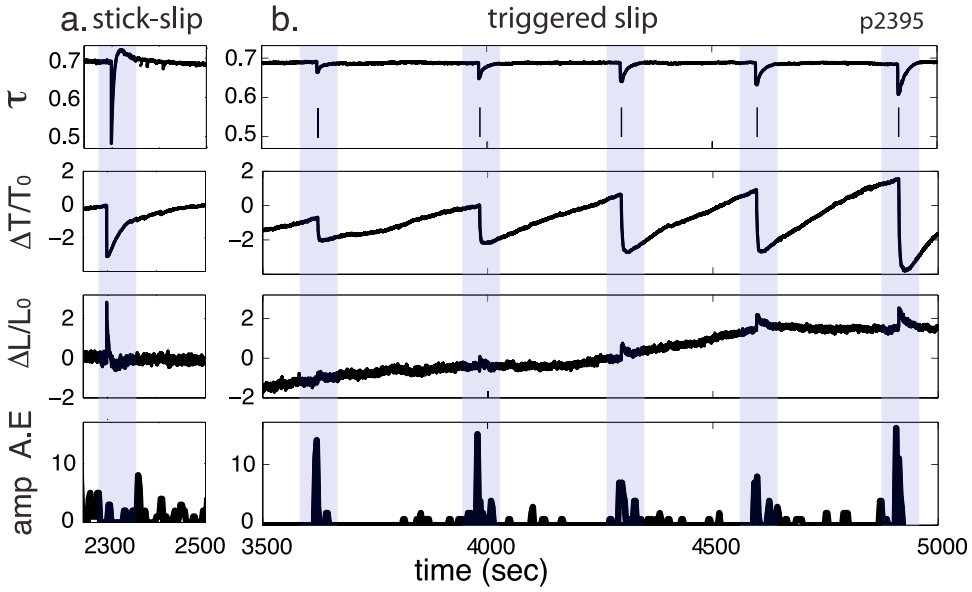

Figure 4. Stick-slip and triggered slow slip for the largest five triggered events for experiment p2395 conducted at 2 MPa horizontal load. In this experiment, the gouge layer begins in stick-slip mode (Figure 4a), evolves to stable sliding where the amplitude dependence measurements were made (Figure 4b), and near the end of the experiment slowly evolves back to stick-slip mode. This sort of instability—stable sliding interspersed with stick-slip, and vice versa—is commonly observed at low applied loads. (a) Example of stick-slip overlain by shadowing. No acoustical perturbation is applied during this time. Curves shown in vertical sequence top to bottom are: shear stress τ in MPa; normalized values of change in gouge layer thickness $\Delta T/T_0$; change in slip along shearing direction $\Delta L/L_0$ obtained from the displacement of the central block (data are detrended, thereby eliminating the effect of the 5 μm/s shearing rate); and detected low-amplitude acoustic emission (AE) in relative amplitude. Each vertical line corresponds to an AE, and the line height corresponds to relative amplitude (relative to the other events). Stick-slips generate large amplitude acoustical radiation by at least one order of magnitude and are not shown so that the AE can be distinguished. The reference values of T_0 and L_0 are the thickness and displacement prior to the slip event. (b) Experimental observations of dynamically triggered, slow slip, induced at progressively larger wave amplitudes during the same experiment. The vertical scales and variables in Figures 4a and 4b are identical. Dynamic-wave triggering of slow slip is indicated by thin vertical lines located beneath the shear stress curves showing triggering times, shown by shadowed regions. Recorded strains of the applied perturbing wave range from 0.5–1.6 microstrain are much larger in amplitude than the AE and are not shown so that the AE events can be distinguished. The recovery of the thickness change due to triggering has a different character than for stick-slip (curves 2a and 2b) indicating that the nature of the dilation responsible for the recovery is different. In both cases, recovery to the original equilibrium thickness occurs, given sufficient time.

of the apparatus. This is a much slower rate than the effects due to wave perturbation).

[9] Figure 2 shows the shear stress of an experiment that exhibits long-duration stable sliding over >1500 s at 2 MPa horizontal stress. Preceding the stable sliding, the material exhibits stick-slip as shown. During the period of stable sliding, acoustical signal bursts (tonebursts) are applied at successively increasing amplitudes. Each detected triggering strain amplitude is shown in Figure 3 as well as the associated shear stress drop signaling a slow slip failure. The shear stress decrease is proportional to the detected strain amplitude and increases as wave strain amplitude increases. We will quantify this relation later. An example of a single, triggered slow slip is shown in Figure 3. Figure 3a shows the detected acoustical toneburst waveform (with expanded view in inset) and Figure 3b shows the effect of the perturbation on the shear stress. The shear stress exhibits characteristic behaviors as noted by Roman numerals in Figure 3b. These are (I) an immediate decrease in frictional strength with an acceleration of shear slip within the gouge layer; (II) a deceleration of slip rate; (III) a stablization in shear stress toward a new equilibrium value until the toneburst signal is terminated (termed material 'conditioning', [e.g., *Guyer and Johnson*, 2009]; (IV) a quasi-elastic recovery; and (V) a material strengthening as the gouge material dilates. Eventually, the shear stress recovers to its pre-triggered level, if one waits long enough (see Figure 2). The induced stress drop and slip event do not produce the large-amplitude acoustical wave radiation associated with laboratory earthquakes, including triggered laboratory earthquakes [*Johnson et al.*, 2008]; however small amplitude acoustic emission (AE) are observed during and following slow slip events (discussed in Figures 4 and 5). Stages (I-V) resemble nonlinear-dynamical behaviors observed in unsheared granular solids [*Guyer and Johnson*, 2009; *Ten Cate and Shankland*, 1996] and unconsolidated, unsheared

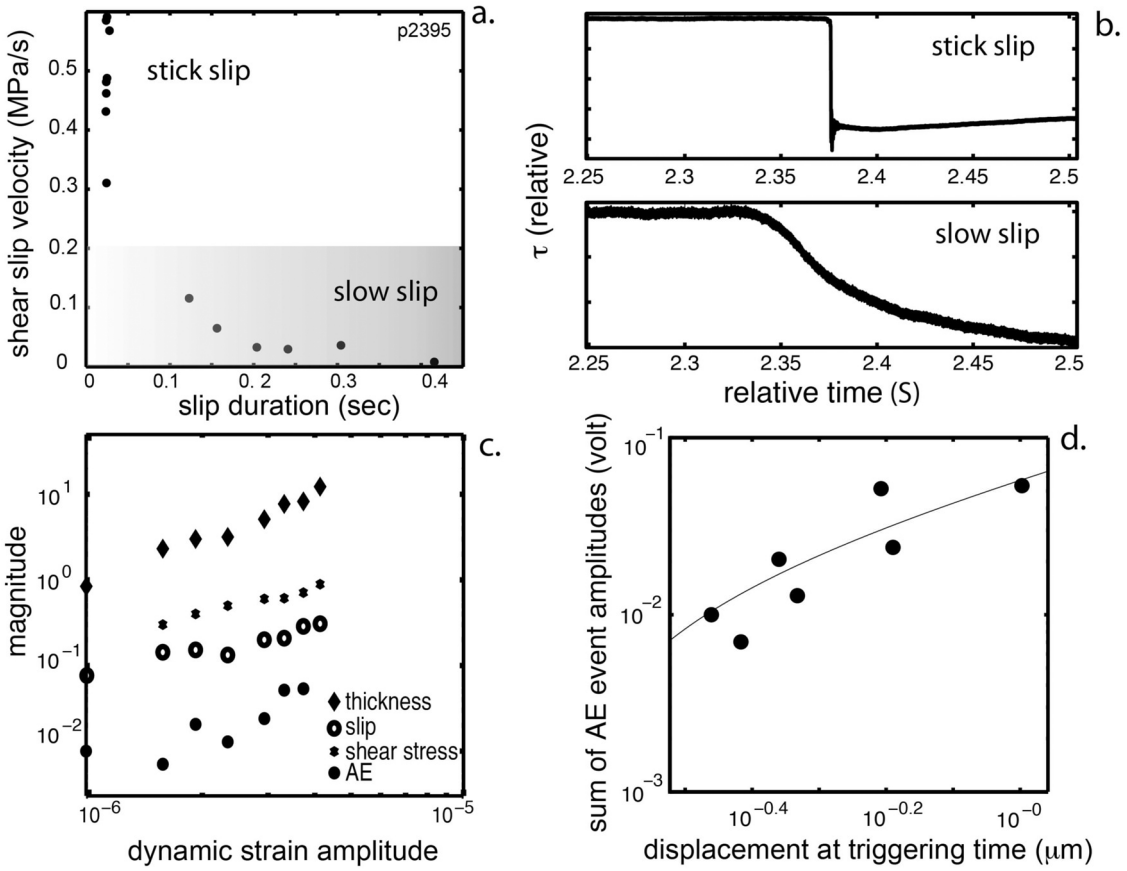

Figure 5. Measured slow slip characteristics. (a) Slip velocity versus slip duration for stick-slip and slow slip events shown in Figure 4. The stick-slip events are shorter in duration than the slow slips. The distribution of slow slip durations are correlated with applied amplitude—in general, the larger the amplitude the longer the slip duration. The average slip velocity reported is obtained from the change in slip corresponding to the stress drop onset minus the change in slope at the end of the event divided by the associated time interval, $\Delta v/\Delta t$. (b) Comparison of a stick slip and slow slip event over the same time interval (shear stress τ is in arbitrary units). At no point in the slow slip event does the slip velocity approach the stick slip velocity. (c) Dependencies of measured parameters on strain amplitude due to triggering wave amplitude. The normalized shear displacement (microns), the thickness change (microns), the shear stress change (MPa) and the sum of the AE amplitudes for 55 s after the slip event (the approximate recovery time) are shown. The sum of the AE amplitudes has a dependence that is very similar to the AE event counts during this same period time. All parameters increase with the applied dynamic strain amplitude, indicating an elastically nonlinear process. (d) Dependence of sum of the AE amplitudes on the slip event distance. A linear function fits the data reasonably well, but the functionality may be different. Note that for the lowest strain amplitude triggering strains (not shown), no change in displacement is measured

glass bead packs [*Johnson and Jia*, 2005; *Brunet et al.*, 2008]. Slow dynamics, the recovery process associated with dilation after wave excitation are analogous to creep, but are driven by a dynamic wave perturbation.

[10] In Figure 4a we show typical stick-slip characteristics and in Figure 4b we show slow slip event characteristics. Slip events of both types are characterized by abrupt shear-stress decrease, layer compaction, shear displacement and AE from the simulated fault zone. The large amplitude broadcast due to the stick-slip event is excluded from Figure 4a in order to show the small amplitude AE, and to compare to the triggered AE. Similarly, the applied triggering toneburst is excluded from the slow slips.

[11] Triggered slip exhibits unique characteristics (Figure 4b): (i) the slip magnitude, stress drop and thickness change are dynamic wave amplitude-dependent; (ii) the stress drop and thickness-change decelerate during slip, extending slip duration (Figure 5a); (iii) bursts of AE occur with triggering, decaying in amplitude and intensity over time; and (iv), the shear stress and material thickness recover to their equilibrium values over tens of seconds (the thickness taking longer to recover).

[12] Figure 5a shows the slip duration versus the shear-slip velocity for stick slips and triggered slow slips, and Figure 5b compares a single stick slip to a slow slip event. The slip initiation is defined as the onset of the shear stress

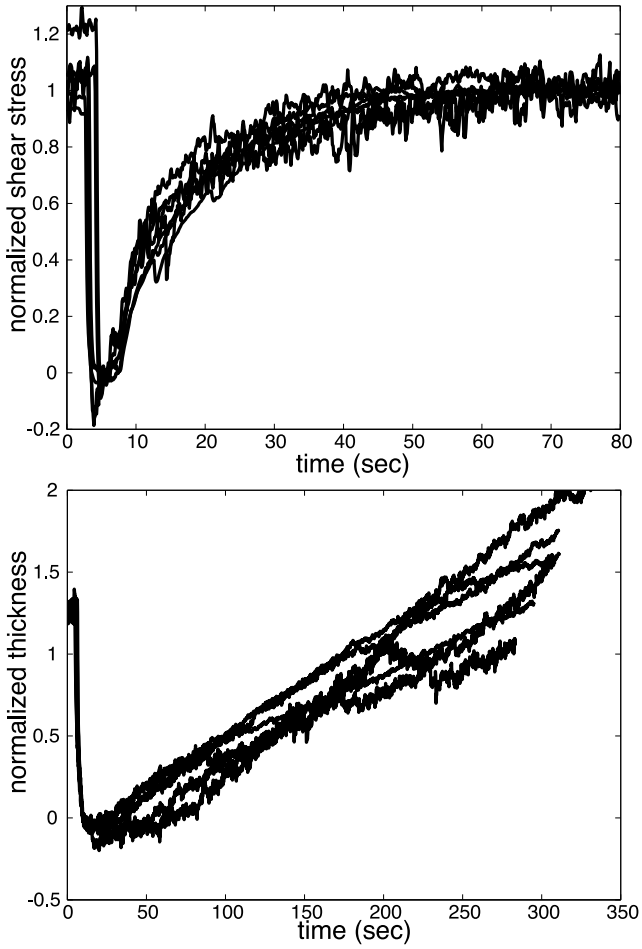

Figure 6. Slow dynamical recoveries of the shear modulus and thickness for the seven triggering events shown in Figure 2. Data have been normalized for overlay. Note approximately exponential recovery of the shear stress and the linear recovery of the thickness, with longer duration. The shear stress curves are normalized such that the average shear stress while sound is applied is zero, and the final average recovered value of the shear stress is 1. The thickness curves are normalized such that the thickness evolves approximately from 1 to zero during the application of the AC signal.

drop and the slip termination is defined by the change in slope of the shear stress at its termination, applying a polynomial fit. For triggered events, the termination of the slip event is defined as the slope change from phases II to III in Figure 3b. The slip duration is clearly longer for the slow slips. Figure 5c shows perturbing wave strain amplitude dependence on the slip characteristics. The approximate linear dependences, the modulus decrease associated with application of dynamic waves (Figure 5c), and long-duration material recovery (Figure 3b) are hallmarks of nonlinear dynamics observed in unsheared glass bead packs and nearly all Earth materials [*Johnson and Jia*, 2005; *Guyer and Johnson*, 2009; *Ten Cate and Shankland*, 1996; *Brunet et al.*, 2008]. Figure 5d shows the relation between the displacement along the shearing direction and the sum of the AE amplitudes occurring during the recovery time (the slow dynamics). There is a clear relation of slip magnitude and the AE intensity. We fit this with a linear function as noted in Figure 5d, but the functionality may be different. The observed amplitude dependence indicates that the triggering is induced by a dynamically elastic nonlinear mechanism—*a dynamically elastic linear mechanism would not result in amplitude dependent parameters.* Mohr-Coulomb failure is one such elastically linear mechanism. During Mohr-Coulomb failure, a wave with stress amplitude sufficiently large would force failure. Larger wave amplitudes would have no additional effect—there would exist no wave amplitude dependence of the measured characteristics shown in Figure 5. We note that we have conducted several other experiments where triggering is induced during stable sliding, including progressively stepping up and down in applied triggering wave amplitude. The results show similar characteristics to those shown in Figure 4.

[13] Figure 6 shows the recoveries—the slow dynamics associated with layer dilation—of the shear stress and the layer thickness, post triggered slip and after the dynamic wave forcing has been terminated. The shear stress and thickness have been normalized for comparison. The recovery of the shear stress appears to be a simple exponential involving a time scale that is independent of the perturbing wave amplitude and/or the size of the shear stress recovery. The recovery process is capacitor-like—the time scale of the recovery is independent of the size of the recovery. The slow dynamical recovery in unsheared sandstone subject to progressively increasing amplitude wave perturbation shows similar recovery behavior [*TenCate et al.*, 2000]. The recovery of the layer thickness, approximately linear in time, is far longer than the shear stress for reasons we currently do not understand; however, in experiments in an unsheared glass bead pack perturbed by an acoustic wave, we also observe longer-term recovery of the material length than the velocity/modulus.

[14] As a means to summarize findings, Figure 7 shows a schematic of the sheared, gouge material elastic response to wave perturbation. We are currently conducting molecular dynamical modeling studies of shear with and without triggering in granular materials in order to quantify the physics controlling the experimental observations [e.g., *Griffa et al.*, 2011, 2012].

4. Analysis and Discussion

[15] Dynamically triggered slow slip has been directly observed in Earth applying GPS, strain and or tilt measurements [e.g., *Glowacka et al.*, 2002; *Bodin et al.*, 1994; *Hudnut and Clark*, 1989; Zigone et al., submitted manuscript, 2012]. Assuming that tremor is a manifestation of slow slip [e.g., *Hiramatsu et al.*, 2008; *Gomberg*, 2010], observations of slow slip and triggered slow slip are becoming increasingly common as more and more observations are made. Dynamically triggered tremor and low frequency earthquakes (LFEs) have been observed in both subduction [e.g., *Miyazawa and Brodsky*, 2008] and transform faulting (the San Andreas fault [e.g., *Shelly*, 2010; *Shelly et al.*, 2011; *Rubinstein et al.*, 2007]). LFEs are discrete signals contained within tremor records that resemble earthquake signals, but which are depleted in higher frequencies when compared to earthquakes of similar

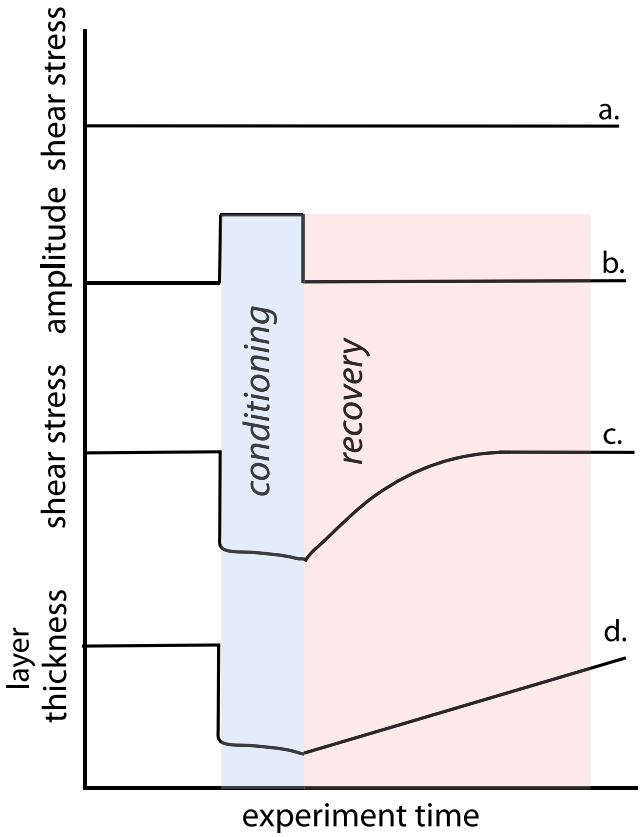

Figure 7. Schematic of the gouge elastic response without and with wave perturbation. (a) Shear stress versus time in the stable sliding regime. (b) Experimental protocol of applying a wave perturbation. (c) Shear stress versus time. (d) Layer thickness versus time. All parameters decrease at the onset of wave perturbation, are subsequently 'conditioned' keeping the respective parameters at a new equilibrium condition, and then recover to their previous equilibrium states after the wave perturbation.

magnitude [*Shelly et al.*, 2011; *Hiramatsu et al.*, 2008]. Tremor and slow slip are coincident where triggered tremor has been observed, such as in Cascadia [*Wech and Creager*, 2007], Japan [*Hiramatsu et al.*, 2008; *Itaba and Ando*, 2011], and the Guerrero region in Mexico (Zigone et al., submitted manuscript, 2012), and has been inferred along the San Andreas Fault at Parkfield [*Brenguier et al.*, 2008; *Shelly et al.*, 2011]. *Shelly et al.* [2011] identified widespread triggering of tremor/LFEs at Parkfield in response to a large number of distant earthquakes. Delayed and long-duration tremor/LFE activity was noted, and the authors infer that the delay and duration point to triggered slow slip as being responsible. Tremor and slow slip have also been shown to be coincident in laboratory studies [*Voisin et al.*, 2008].

[16] The relation between AE integrated event amplitudes and slip magnitude observed in the laboratory shown in Figure 5c indicates that (i) AE bursts are due to triggered slow slip, (ii) that AE is a proxy for slip, (iii) that the slip magnitude is wave amplitude dependent and (iv) that the gouge compacts at triggered slip time (Figure 5b). We posit the laboratory AE are a manifestation of a similar process as that in Earth, and that the LFEs/tremor are a proxy for slip.

[17] Our work suggests that triggered slow slip and LFEs/tremor occur only at extremely low effective pressures—lower than those necessary to trigger laboratory earthquakes. In fact we have induced triggered slow slip early in the shear stress cycle where material dilation is only beginning (Figure 8) in accord with some Earth observations [*Hudnut and Clark*, 1989] but in contrast to others [*Gomberg*, 2010]. Triggering of stick-slip is observed only when the material is in a critical state, near failure [*Johnson et al.*, 2008]. The experimental work suggests that triggering of all types of slip by dynamic waves requires small effective pressures. At 2 MPa, assuming a density of 2 kg/m^3 and a wave speed of 1000 m/s, and dynamic strains $\varepsilon = 10^{-6}$–10^{-5}, acoustical pressures induced in the laboratory study are of order

$$P_{dyn} = \rho c^2 \varepsilon = \sim 20 - 200 \ \mathrm{N/m^2} \sim 20 - 200 \ \mathrm{Pa}. \quad (2)$$

This is $10^{-7} - 10^{-6}$% of the applied horizontal stress. As effective pressure increases, the acoustic pressures become a smaller fraction of the applied pressure and the elastic nonlinearity has a correspondingly smaller effect. At effective stresses of about 30 MPa, nonlinear effects in rock are unmeasureable [e.g., *Zinszner et al.*, 1997], supporting the hypothesis that effective pressures must be very low for nonlinear dynamical triggering to take place.

[18] Triggering of this nature takes place *because* of the nonlinear dynamics of the gouge, which forces simultaneous shear stress decrease and layer compaction inducing a slip event. We believe that it is the nonlinear 'conditioning' of the material that modifies and destabilizes its elastic properties, preparing it for and acting during slip. The waves destabilize the material during stable sliding, forcing a shear stress drop, layer compaction and slip event. This

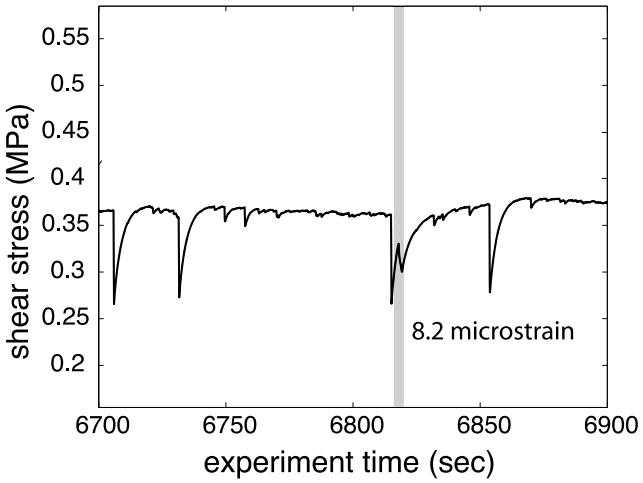

Figure 8. Triggering of slow slip early in the stress cycle at 1 MPa. An acoustic wave of about 1 s duration and a recorded amplitude of 8.2 microstrain is applied early in the slip cycle. The perturbation induces the slow slip event noted by the shaded region. The observation is highly repeatable. At loads >∼3 MPa, we have not observed triggered slip of any kind in glass beads unless the granular material is in a critical state, near failure (within the wave dynamic strains applied (10^{-9}–10^{-5})).

interpretation is also suggested by experiments applying rotary shear of glass beads by N. J. van der Elst et al. (Auto-acoustic compaction in steady shear flows: Experimental evidence for suppression of shear dilatancy by internal acoustic vibration, submitted to *Journal of Geophysical Research*, 2011). This work shows that as granular media begins to flow, noise created by grain collisions induces compaction. Thus when an external dynamic perturbation begins the triggering process the grain interactions themselves may help sustain slip.

[19] Our results show that laboratory stick-slip and slow slip result in material compaction during slip that differs from the commonly applied rate and state friction model [e.g., *Dieterich*, 1978]. In our experiments, the compaction occurs during stick-slip (Figure 4a), triggered stick-slip [*Johnson et al.*, 2008] and triggered slow slip (Figure 4b), while the rate and state models predict material dilation during slip. Rate-state model results [e.g., *Segall and Rice*, 1995] are based on velocity step experiments by one of the authors (Marone) [*Marone*, 1998] applying the same experimental apparatus used in the experiments described here. Velocity steps represent a very different loading condition than those used in stick-slip experiments, and consequently rate and state models may require revision to be consistent with our experimental data. Nonlinear dynamics are not accounted for in the rate-state model. Discrete Element Modeling by *Griffa et al.* [2011, 2012] also shows that the material bulk compacts with the shear-stress drop. Our studies quantitatively show that the evolution of thickness during both stick and slip portions of the stick-slip cycle is closely tied to the dynamics, which could provide improved constraints on friction laws.

[20] Our work also illustrates that fluids are neither a necessary ingredient in triggering of slow slip, nor a required part of triggered stick-slip. Low effective stress or a weak fault [*Zoback and Beroza*, 1993] is required for triggering of slow slip and stick slip, and fluids certainly are one manner to reduce effective stress.

5. Conclusions

[21] In summary, our laboratory observations show that slow slip may be triggered by nonlinear dynamics. We posit that triggered slow slip may be due to dynamic waves inducing gouge material deformation [*Tordesillas and Behringer*, 2009] forcing instability and force chain collapse [*Griffa et al.*, 2011, 2012]. The compaction, modulus decrease and successive recovery—the slow dynamics—are the characteristics of elastic nonlinearity. While the experiments represent a highly idealized fault relative to Earth, we observe similar observations in Earth, implying that there are aspects of the triggering process in the laboratory experiments that scale. Finally, we do not suggest that nonlinear dynamics are the only potential mechanism of triggered slow slip nor triggered slip in general, but that they represent a strong candidate for one mechanism of triggered failure.

[22] **Acknowledgments.** This work was supported by Institutional Support (LDRD) at Los Alamos National Laboratory and NSF grants OCE 0648331 and NSF-EAR0911569 to CM. We thank Jan Carmeliet, Michele Griffa, Behrooz Ferdowsi, Robert Guyer, Joan Gomberg, Emily Brodsky, David Shelly, Michel Campillo, Dimitri Zigone, Stefan Nielsen and Diane Rivet for discussions.

References

Allen, C. R., M. Wyss, J. N. Brune, A. Granz, and R. Wallace (1972), Displacements on the Imperial, Superstition Hills, and San Andreas faults triggered by the Borrego Mountain Earthquake, *The Borrego Mountain Earthquake*, *U.S. Geol. Surv. Prof. Pap.*, *787*, 87–104.

Bodin, P., R. Bilham, J. Behr, J. Gomberg, and K. Hudnut (1994), Slip triggered on Southern California faults by the 1992 Joshua Tree, Landers, and Big Bear Earthquakes, *Bull. Seismol. Soc. Am.*, *84*, 806–816.

Brenguier, F., M. Campillo, C. Hadziioannou, N. Shapiro, R. M. Nadeau, and E. Larose (2008), Postseismic relaxation along the San Andreas Fault at Parkfield from continuous seismological observations, *Science*, *321*, 1478–1481, doi:10.1126/science.1160943.

Brodsky, E., and S. G. Prejean (2005), New constraints on mechanisms of remotely triggered seismicity at Long Valley Caldera, *J. Geophys. Res.*, *110*, B04302, doi:10.1029/2004JB003211.

Brunet, T., X. Jia, and P. A. Johnson (2008), Transitional nonlinear elastic behaviour in dense granular media, *Geophys. Res. Lett.*, *35*, L19308, doi:10.1029/2008GL035264.

Dieterich, J. H. (1978), Time-dependent friction and the mechanics of stick-slip, *Pure Appl. Geophys.*, *116*, 790–806, doi:10.1007/BF00876539.

Glowacka, E., F. Alehandro Nava, G. Diaz de Cossio, V. Wong, and F. Farfan (2002), Fault slip, seismicity, deformation in Mexacali Calley, Baja, California, Mexico, after the M 7.1 1999 Hector Mine Earthquake, *Bull. Seismol. Soc. Am.*, *92*, 1290–1299, doi:10.1785/0120000911.

Gomberg, J. (2001), The failure of earthquake failure models, *J. Geophys. Res.*, *106*, 16,253–16,263, doi:10.1029/2000JB000003.

Gomberg, J. (2010), Lessons from (triggered) tremor, *J. Geophys. Res.*, *115*, B10302, doi:10.1029/2009JB007011.

Gomberg, J., and P. A. Johnson (2005), Seismology: Dynamic triggering of earthquakes, *Nature*, *437*, 830–832, doi:10.1038/437830a.

Gomberg, J., M. L. Blanpied, and N. M. Beeler (1997), Transient triggering of near and distant earthquakes, *Bull. Seismol. Soc. Am.*, *87*, 294–309.

Gomberg, J., P. Bodin, and P. A. Reasenberg (2003), Observing earthquakes triggered in the near field by dynamic deformations, *Bull. Seismol. Soc. Am.*, *93*, 118–138, doi:10.1785/0120020075.

Gomberg, J., P. Bodin, K. Larson, and H. Dragert (2004), Earthquake nucleation by transient deformations caused by the M = 7.9 Denali, Alaska earthquake, *Nature*, *427*, 621–624, doi:10.1038/nature02335.

Gonzalez-Huizar, H., and A. A. Velasco (2011), Dynamic triggering: Stress modeling and a case study, *J. Geophys. Res.*, *116*, B02304, doi:10.1029/2009JB007000.

Griffa, M., E. Daub, R. Guyer, P. A. Johnson, C. Marone, and J. Carmeliet (2011), Vibration-induced unjamming of sheared granular layers and the micromechanics of dynamic earthquake triggering, *Europhys. Letters*, *96*, 14001, doi:10.1209/0295-5075/96/14001.

Griffa, M., B. Ferdowsi, E. G. Daub, R. A. Guyer, P. A. Johnson, C. Marone, and J. Carmeliet (2012), Meso-mechanical analysis of deformation characteristics for dynamically triggered slip in granular materials, *Philos. Mag.*, in press.

Guyer, R. A., and P. A. Johnson (2009), *Nonlinear Mesoscopic Elasticity: The Complex Behaviour of Rocks and Soil*, Wiley-VCH, Berlin.

Hawthorne, J. C., and A. M. Rubin (2010), Tidal modulation of slow slip in Cascadia, *J. Geophys. Res.*, *115*, B09406, doi:10.1029/2010JB007502.

Hiramatsu, Y., T. Wanatabe, and K. Obara (2008), Deep low-frequency tremors as a proxy for slip monitoring at plate interface, *Geophys. Res. Lett.*, *35*, L13304, doi:10.1029/2008GL034342.

Hudnut, K. W., and M. M. Clark (1989), New slip along parts of the 1968 Coyote Creek fault rupture, California, *Bull. Seismol. Soc. Am.*, *79*, 451–465.

Itaba, S., and R. Ando (2011), A slow slip event triggered by teleseismic surface waves, *Geophys. Res. Lett.*, *38*, L21306, doi:10.1029/2011GL049593.

Johnson, P. A., and X. Jia (2005), Nonlinear dynamics, granular media and dynamic earthquake triggering, *Nature*, *437*, 871–874, doi:10.1038/nature04015.

Johnson, P. A., H. Savage, M. Knuth, J. Gomberg, and C. Marone (2008), The effect of acoustic waves on stick-slip behavior in sheared granular media: Implications for earthquake recurrence and triggering, *Nature*, *451*, 57–60, doi:10.1038/nature06440.

Marone, C. (1998), Laboratory-derived friction laws and their application to seismic faulting, *Annu. Rev. Earth Planet. Sci.*, *26*, 643–696, doi:10.1146/annurev.earth.26.1.643.

Marsan, D., and I. Lengliné (2008), Extending earthquakes' reach through cascading, *Science*, *319*, 1076–1079, doi:10.1126/science.1148783.

Miyazawa, M., and E. E. Brodsky (2008), Deep low-frequency tremor that correlates with passing surface waves, *J. Geophys. Res.*, *113*, B01307, doi:10.1029/2006JB004890.

Miyazawa, M., and J. Mori (2005), Detection of triggered deep low-frequency events from the 2003 Tokachi-oki earthquake, *Geophys. Res. Lett.*, *32*, L10307, doi:10.1029/2005GL022539.

Peng, Z., and J. Gomberg (2010), An integrated perspective of the continuum between earthquakes and slow slip phenomena, *Nat. Geosci.*, *3*, 599–607, doi:10.1038/ngeo940.

Rogers, G., and H. Dragert (2003), Episodic tremor and slip on the Cascadia Subduction Zone: The chatter of silent slip, *Science*, *300*, 1942–1943, doi:10.1126/science.1084783.

Rubinstein, J., J. Vidale, J. Gomberg, P. Bodin, K. Creager, and S. D. Malone (2007), Non-volcanic tremor driven by large transient shear stresses, *Nature*, *448*, 579–582, doi:10.1038/nature06017.

Rubinstein, J. R., D. R. Shelly, and W. L. Ellsworth (2010), Non-volcanic tremor: A window into the roots of fault zones, in *New Frontiers in Integrated Solid Earth Sciences*, pp. 287–314, Springer, New York, doi:10.1007/978-90-481-2737-5_8.

Scholz, C. (2010), Large earthquake triggering, clustering and the synchronization of faults, *Bull. Seismol. Soc. Am.*, *100*, 901–909, doi:10.1785/0120090309.

Segall, P., and J. R. Rice (1995), Dilatancy, compaction, and slip instability of a fluid-infiltrated fault, *J. Geophys. Res.*, *100*, 22,155–22,171, doi:10.1029/95JB02403.

Shelly, D. (2010), Migrating tremors illuminate complex deformation beneath the seismogenic San Andreas fault, *Nature*, *463*, 648–652, doi:10.1038/nature08755.

Shelly, D., Z. Peng, D. Hill, and C. Aiken (2011), Triggered creep as a possible mechanism for delayed dynamic triggering of tremor and earthquakes, *Nat. Geosci.*, *4*, 384–388, doi:10.1038/ngeo1141.

Sornette, A., and D. Sornette (1989), Self-organized criticality and earthquakes, *Europhys. Lett.*, *9*, 197–202, doi:10.1209/0295-5075/9/3/002.

Taira, T., P. G. Silver, F. Niu, and R. M. Nadeau (2009), Remote triggering of fault-strength changes on the San Andreas fault at Parkfield, *Nature*, *461*, 636–639, doi:10.1038/nature08395.

Ten Cate, J. A., and T. J. Shankland (1996), Slow dynamics in the nonlinear elastic response of Berea sandstone, *Geophys. Res. Lett.*, *23*, 3019–3022, doi:10.1029/96GL02884.

TenCate, J. A., E. Smith, and R. Guyer (2000), Universal slow dynamics in granular solids, *Phys. Rev. Lett.*, *85*, 1020–1023, doi:10.1103/PhysRevLett.85.1020.

Tordesillas, A., and B. Behringer (2009), Buckling force chains in dense granular assemblies: Physical and numerical experiments, *Geomech. Geoeng.*, *4*, 3–16, doi:10.1080/17486020902767347.

van der Elst, N. J., and E. Brodsky (2010), Connecting near and farfield triggering to dynamic strain, *J. Geophys. Res.*, *115*, B07311, doi:10.1029/2009JB006681.

Voisin, C., J.-R. Grasso, E. Larose, and F. Renard (2008), Evolution of seismic signals and slip patterns along subduction zones: Insights from a friction lab scale experiment, *Geophys. Res. Lett.*, *35*, L08302, doi:10.1029/2008GL033356.

Wech, A. G., and K. C. Creager (2007), Cascadia tremor polarization evidence for plate interface slip, *Geophys. Res. Lett.*, *34*, L22306, doi:10.1029/2007GL031167.

Zinszner, B., P. A. Johnson, and P. N. J. R. Rasolofosaon (1997), Influence of change in physical state on elastic nonlinear response in rock: Effects of confining pressure and saturation, *J. Geophys. Res.*, *102*, 8105–8120, doi:10.1029/96JB03225.

Zoback, M. D., and G. Beroza (1993), Evidence for near-frictionless faulting in the 1989 (M 6.9) Loma Prieta, California, earthquake and its aftershocks, *Geology*, *21*, 181–185, doi:10.1130/0091-7613(1993)021<0181:EFNFFI>2.3.CO;2.

B. Carpenter, B. M. Kaproth, and C. Marone, Department of Geosciences, Pennsylvania State University, University Park, PA 16802, USA.

E. G. Daub, P. A. Johnson, and P.-Y. Le Bas, Geophysics Group, Los Alamos National Laboratory, Los Alamos, NM 87545, USA. (paj@lanl.gov)

M. Knuth, Department of Geology and Geophysics, University of Wisconsin-Madison, Madison, WI 53706, USA.